Efficient capture of C2H2 from CO2 and CnH4 by a novel fluorinated anion pillared MOF with flexible molecular sieving effect

Wang, L.; Xu, N.; Hu, Y.; Sun, W.; Krishna, R.; Li, J.; Jiang, Y.; Duttwyler, S.; Zhang, Y.

DOI
10.1007/s12274-022-4996-9

Publication date
2023

Document Version
Final published version

Published in
Nano Research

Research Article

Nano Research
2023, 16(2): 3536–3541

ISSN 1998-0124 CN 11-5974/O4
https://doi.org/10.1007/s12274-022-4996-9

Efficient capture of C_2H_2 from CO_2 and C_nH_4 by a novel fluorinated anion pillared MOF with flexible molecular sieving effect

Lingyao Wang[1], Nuo Xu[1], Yongqi Hu[1], Wanqi Sun[1], Rajamani Krishna[2], Jiahao Li[1], Yunjia Jiang[1], Simon Duttwyler[3], and Yuanbin Zhang[1] (✉)

[1] *Key Laboratory of the Ministry of Education for Advanced Catalysis Materials, College of Chemistry and Life Sciences, Zhejiang Normal University, Jinhua 321004, China*
[2] *Van't Hoff Institute for Molecular Sciences, University of Amsterdam, Science Park 904, Amsterdam 1098 XH, the Netherlands*
[3] *Department of Chemistry, Zhejiang University, Hangzhou 310027, China*

Received: 12 July 2022 / **Revised:** 11 August 2022 / **Accepted:** 31 August 2022

ABSTRACT

The efficient separation of acetylene (C_2H_2) from carbon dioxide (CO_2) and C_nH_4 (n = 1 and 2) to manufacture high purity C_2H_2 and recover other light hydrocarbons is technologically important, while posing significant challenges. Herein, we reported a new TiF_6^{2-} anion (TIFSIX) pillared metal-organic framework (MOF) ZNU-5 (ZNU = Zhejiang Normal University) with ultramicropores for highly selective C_2H_2 capture with low adsorption heat through gate opening based molecular sieving effect. ZNU-5 takes up a large amount of C_2H_2 (128.6 cm^3/g) at 1.0 bar and 298 K but excludes CO_2, CH_4, and C_2H_4. Such high capacity has never been realized in MOFs with molecular sieving. The breakthrough experiments further confirmed the highly selective C_2H_2 separation performance from multi-component gas mixtures. 3.3, 2.8, and 2.2 mmol/g of C_2H_2 is captured at ZNU-5 from equimolar C_2H_2/CO_2, $C_2H_2/CO_2/CH_4$, and $C_2H_2/CO_2/CH_4/C_2H_4$ mixtures, respectively. Furthermore, 2.6, 2.0, and 1.5 mmol/g of > 98% purity C_2H_2 can be recycled from the desorption process. Combining high working capacity, low adsorption heat, as well as good recyclability, ZNU-5 is promising for C_2H_2 purification.

KEYWORDS

metal-organic frameworks (MOFs), C_2H_2/CO_2 separation, acetylene recovery, molecular sieving, flexible MOFs

1 Introduction

Acetylene (C_2H_2) is a major raw feedstock for the production of various essential chemicals and polymers in industry [1–3]. It is produced from the partial combustion of natural gas or stream cracking of hydrocarbons, in which carbon dioxide (CO_2) and other C_1-C_2 light hydrocarbons are worth-noting contaminants that need to be removed to produce C_2H_2 in high purity [4, 5]. Currently, energy-intensive cryogenic distillation and solvent extraction are employed for the recovery of C_2H_2 from other gases. Due to the close boiling points, these approaches suffer from low energy inefficiency and are environmentally unfriendly. Therefore, physisorptive separation using porous solid adsorbents has attracted particular interest based on the lower cost and energy consumption [6–16]. However, the similarities among these gas molecules in terms of molecular size (kinetic diameter: 3.3 Å for both C_2H_2 and CO_2, 3.8 Å for CH_4, and 4.2 Å for C_2H_4) and physical properties make these separations a great challenge [17–21].

Metal-organic frameworks (MOFs) are famous for their powerful structural predictability and tunability on pore size/shape and functionality [22–30]. However, the flexibility of MOFs is still very challenging to predict and flexible MOFs have less been studied in selective gas separation. UTSA-300 (SIFSIX-dps-Zn; SIFSIX = SiF_6^{2-}, dps = 4,4′ -dipyridylsulfide) [31] is the first reported flexible MOF that takes up 69.0 cm^3/g of C_2H_2 and negligible CO_2 and C_2H_4. By replacing the zinc ion (Zn^{2+}) to copper ion (Cu^{2+}), the resulting SIFSIX-dps-Cu [32] exhibits increased C_2H_2 uptake of 102.4 cm^3/g as well as an ultrahigh selectivity of 1,787. However, the practical dynamic capacity of C_2H_2 from equimolar C_2H_2/CO_2 mixture is only 2.48 mmol/g, even lower than that (2.9 mmol/g) of our recently reported robust MOF ZNU-1 (ZNU = Zhejiang Normal University) [33] with static uptake of 76.3 cm^3/g and ideal adsorbed solution theory (IAST) selectivity of 56.6. Therefore, high practical working capacity is still very difficult to realize by flexible MOFs in the context of challenging C_2H_2/CO_2 separation.

Herein, we would like to report a new TiF_6^{2-} anion (TIFSIX) pillared flexible metal-organic framework ZNU-5 for selective C_2H_2 adsorption. ZNU-5 is constructed by self-assembly of $CuTiF_6$ and 1,4-di(1H-imidazol-1-yl)benzene (DIB) in $MeOH/H_2O$ solution. It displays a large capacity of 128.6 cm^3/g for C_2H_2 under 1.0 bar and 298 K but only adsorbs 15.2, 11.9, and 3.5 cm^3/g of CO_2, C_2H_4, and CH_4. The near-zero coverage C_2H_2 adsorption heat is as low as 27.8 kJ/mol, indicative of its low energy footprint for material regeneration. The calculated IAST selectivities at 1.0 bar are 11.6 for C_2H_2/CO_2, 255 for C_2H_2/C_2H_4, and 850 for C_2H_2/CH_4. Such high selectivities have rarely been achieved by reported top-performing MOFs. The practical separation performance is fully demonstrated by the breakthrough

Address correspondence to ybzhang@zjnu.edu.cn

experiments of multi-component gas mixtures. 3.3, 2.8, and 2.2 mmol/g of C_2H_2 is captured at ZNU-5 from 50/50 C_2H_2/CO_2, 33.3/33.3/33.3 $C_2H_2/CO_2/CH_4$, and 25/25/25/25 $C_2H_2/CO_2/CH_4/C_2H_4$ mixtures, respectively. 2.6, 2.0, and 1.5 mmol/g of > 98% purity C_2H_2 can be recycled from the desorption process. No separation performance reduction is observed over 5 cycles. Therefore, combining high working capacity, low adsorption heat, as well as good recyclability, ZNU-5 is promising for C_2H_2 purification.

2 Experimental

2.1 Synthesis of ZNU-5

To a 5 mL long thin tube was added 1 mL of aqueous solution with $(NH_4)_2TiF_6$ (1 mg) and $Cu(NO_3)_2{\cdot}3H_2O$ (1 mg). 3 mL of MeOH/H_2O mixture was slowly layered above the solution, followed by 1 mL of MeOH solution of 1,4-di(1H-imidazol-1-yl)benzene (2 mg). The tube was sealed and left undisturbed at room temperature. After several days, purple needle-shaped crystals were formed on the glass surface. The average yield was ca. 75%.

2.2 Synthesis of ZNU-4

To a 5 mL long thin tube was added 1 mL of aqueous solution with $(NH_4)_2TiF_6$ (1 mg) and $Cu(NO_3)_2{\cdot}3H_2O$ (1 mg). 2 mL of MeCN/H_2O mixture was slowly layered above the solution, followed by 1 mL of MeCN solution of 1,4-di(1H-imidazol-1-yl)benzene (2 mg). The tube was sealed and left undisturbed at room temperature. After several days, blue flake shaped crystals were formed on the glass surface. The average yield was ca. 75%.

3 Results and discussion

3.1 Structural analysis and characterization

Light blue single crystals of ZNU-4 [34] with zsd topology was prepared in MeCN/H_2O solution (Fig. S2(a) in the Electronic Supplementary Material (ESM)). Each Cu(II) ion of ZNU-4 is connected to four imidazole nitrogen atoms from four different DIB ligands and two fluorine atoms from two TiF_6^{2-} groups (Figs. 1(a) and 1(b)). The DIB ligand is in anti-configuration while TiF_6^{2-} is coordinating through trans mode. Six copper ions and six DIB linkers generate a very twisted loop. Every unit cell contains two adjacent narrow one-dimensional (1D) channel with fluorine atoms decorated in the surface (Fig. 1(c)). The solvents play an important role in the self-assembly of the building units. In MeOH/H_2O solution, needle-shaped purple crystals of ZNU-5 were cultivated with distinct porous structures (Fig. S2(b) in the ESM). As shown in Fig. 1(d), every Cu(II) cation is octahedrally coordinated to four DIB ligands in half syn and half anti configuration and two TIFSIX anions in cis coordination mode, extending to a non-interpenetrated pcu topology framework (Fig. 1(e)). Different from ZNU-4, ZNU-5 features two-dimensional pore channels as shown in Fig. 1(f).

As shown in Fig. 2(a), the powder X-ray diffraction (PXRD) patterns of the as-synthesized ZNU-5 are consistent with the simulated ones from crystal structure, indicating the pure phase of sample. ZNU-5 is relatively stable in humid air but sensitive to water. A new phase appears when the sample is immersed in water. Interestingly, the original phase can be recovered when the water-soaked samples were re-activated or re-soaked in methanol (Fig. S12 in the ESM). Thermo gravimetric analysis (TGA) analysis was conducted to compare the thermal stability of ZNU-4 and ZNU-5 qualitatively (Fig. 2(b)). The weight reduction before 150 °C belongs to the loss of water and organic solvent in the pores. ZNU-5 shows a second weight loss until 340 °C, slightly higher than that of ZNU-4 (290 °C), suggesting the superior thermal stability of ZNU-5.

3.2 Single-component adsorption experiments and selectivity calculations

To evaluate the pore properties of ZNU-4 and ZNU-5, CO_2 adsorption measurements were performed at 195 K (Fig. 3(a)). ZNU-4 displays the type-I isotherm and the maximum loading is 105.7 cm^3/g at 100 kPa. The Brunauer–Emmett–Teller (BET) surface area is 358.6 m^2/g. In contrast, two stages of CO_2 adsorption are observed for ZNU-5. The CO_2 uptakes in the first and second steps are 200.9 (15 kPa) and 299.8 cm^3/g (100 kPa), respectively. The BET surface area is 751.5 m^2/g (Fig. S14(b) in the ESM). The calculated pore width is 5.2 Å (Fig. S14(a) in the ESM), perfectly consistent with the pore size (5.2 Å) measured from the single crystal structure (Fig. S10 in the ESM).

The distinct structure/pore architectures and porosity of ZNU-4 and ZNU-5 prompted us to evaluate their difference in gas

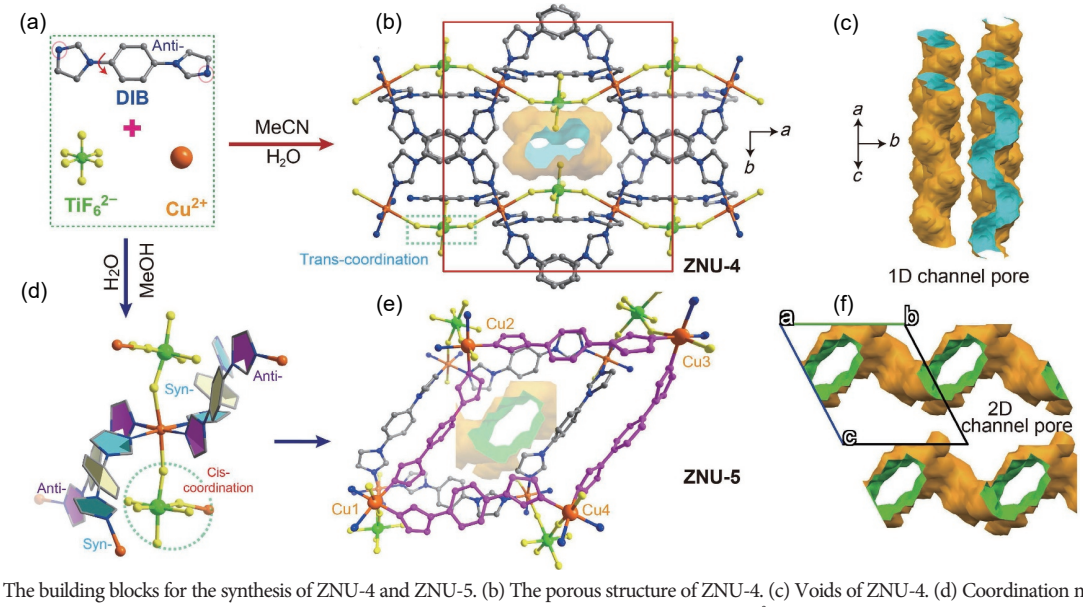

Figure 1 (a) The building blocks for the synthesis of ZNU-4 and ZNU-5. (b) The porous structure of ZNU-4. (c) Voids of ZNU-4. (d) Coordination mode in ZNU-5. (e) The porous structure of ZNU-5. (f) Voids of ZNU-5. The voids are generated by a probe with a radius of 1.2 Å.

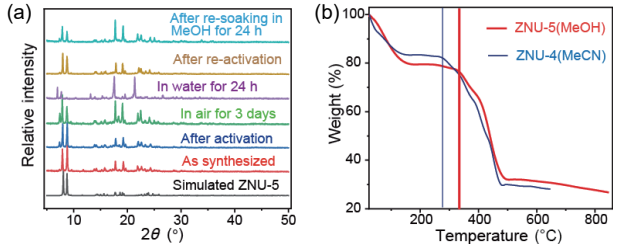

Figure 2 (a) PXRD patterns of ZNU-5 under different condition. (b) Thermo gravimetric analysis curve of ZNU-4 and ZNU-5.

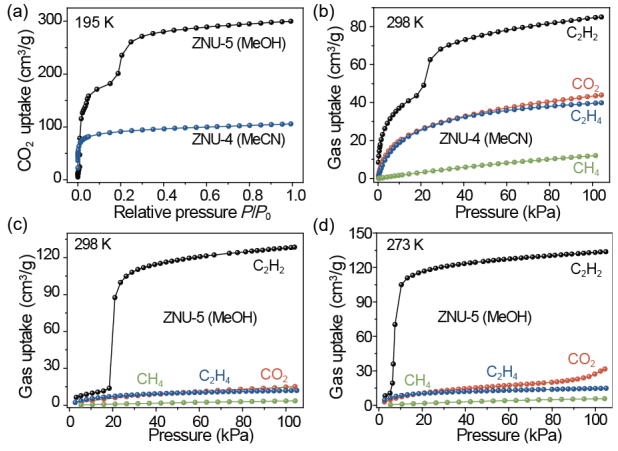

Figure 3 (a) CO_2 adsorption isotherm for ZNU-4 and ZNU-5 at 195 K. (b) C_2H_2, CO_2, C_2H_4, and CH_4 adsorption isotherms in ZNU-4 at 298 K. (c) and (d) C_2H_2, CO_2, C_2H_4, and CH_4 adsorption isotherms in ZNU-5 at 298 and 273 K.

adsorption and separation performances. As shown in Figs. 3(b)–3(d), and Figs. S15 and S16 in the ESM, we performed unary gas adsorption tests for C_2H_2, CO_2, C_2H_4, and CH_4 under the temperature ranging from 263 to 313 K. The C_2H_2 adsorption isotherms of ZNU-5 showed gate-opening pressure increases from 5 kPa (273 K) to around 20 kPa (298 K) and 30 kPa (313 K), indicating that the gate-opening pressure is temperature dependent. Such temperature dependent gate-opening has also been observed for CO_2 at 263 K, which possesses a higher gate-opening pressure (65 kPa). Impressively, ZNU-5 exhibits a remarkably high C_2H_2 uptake of 128.6 cm^3/g at 298 K and 100 kPa with a flexible feature (Fig. 3(c)), which is 51.1% higher than that of ZNU-4 (85.1 cm^3/g). This value sets a new record of C_2H_2 capacity at 100 kPa among MOF materials with C_2H_2/CO_2 molecular sieving effect, which outperforms many benchmark MOFs including UTSA-300 (69.0 cm^3/g) [31], NTU-65 (75.4 cm^3/g) [35], ZJU-196 (83.5 cm^3/g) [36], CPL-1-NH_2 (41.2 cm^3/g) [37], SIFSIX-dps-Cu (102.4 cm^3/g) [32], and MOF-OH (60.0 cm^3/g) [38]. Notably, ZNU-5 completely prevents the CO_2, C_2H_4, and CH_4 entrance at the pressure up to 100 kPa at 298 K. Therefore, the exceptional C_2H_2 capture capacity at 100 kPa combined with the much lower CO_2, C_2H_4, and CH_4 uptakes enables ZNU-5 with great potential to achieve one-step C_2H_2 purification from quaternary $C_2H_2/CO_2/C_2H_4/CH_4$ mixtures.

Figure 4(a) shows that the initial Q_{st} values for C_2H_2 (27.8 kJ/mol) in ZNU-5 is much lower than that of ZNU-4 (50.3 kJ/mol), implying a relatively low energy consumption in regeneration.

IAST calculations were performed to qualitatively evaluate the adsorption selectivity of ZNU-4 and ZNU-5 for equimolar C_2H_2/CO_2, C_2H_2/C_2H_4, and C_2H_2/CH_4 mixtures at 298 K, respectively. Due to the existence of the gate-opening phenomenon, the fitting is challenging and temperature dependant dual-site Langmuir–Freundlich model is applied. The comparison of experimental and simulated adsorption isotherms

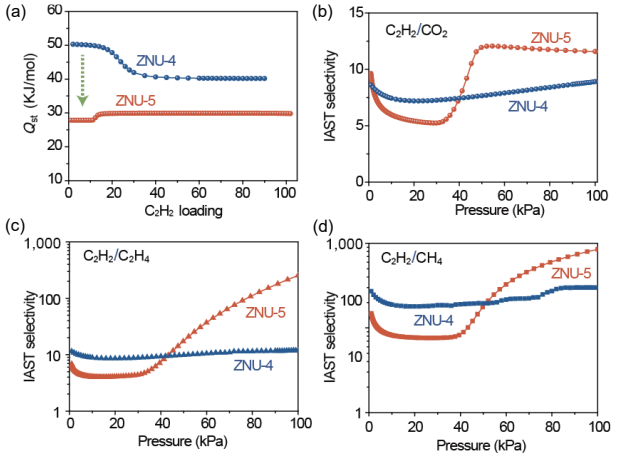

Figure 4 (a) Q_{st} for C_2H_2 adsorption in ZNU-4 and ZNU-5. (b)–(d) IAST selectivity for equimolar C_2H_2/CO_2, C_2H_2/C_2H_4, and C_2H_2/CH_4 mixtures in ZNU-4 and ZNU-5 at 298 K.

as well as the fitting parameters are presented in Fig. S17 and Table S3 in the ESM, which showed the fitting is in excellent accuracy. For equimolar C_2H_2/CO_2, C_2H_2/C_2H_4, and C_2H_2/CH_4 mixtures, as presented in Figs. 4(b)–4(d), ZNU-5 exhibits a higher selectivity up to 12, 255, and 850 at 100 kPa, which is superior to ZNU-4 with the selectivity of 9, 12, and 300.

The comparison of C_2H_2 and CO_2 uptake in top-performing materials is presented in Fig. 5(a). ZNU-5 is the best example that shows a very high C_2H_2 uptake as well as a very low CO_2 uptake, which is also reflected in the C_2H_2/CO_2 uptake ratio in Fig. 5(b). SNNU-65-Cu-Sc [39], MIL-160 [40], FJU-90 [41], SIFSIX-Cu-TPA [42], and SIFSIX-1-Cu [43] exhibited a higher C_2H_2 uptake, yet a higher CO_2 uptake as well, leading to decreased C_2H_2/CO_2 selectivity. Besides, ZNU-5 is the only porous materials that exhibit a C_2H_2/CO_2 uptake ratio > 8 and Q_{st} value < 30 kJ/mol [44–53]. A more comprehensive comparison table is listed in Tables S4–S6 in the ESM, among which ZNU-5 is still a benchmark material for C_2H_2 recovery from other gases.

3.3 Dynamic breakthrough experiments

Transient breakthrough simulations were conducted to evaluate the separation performance of ZNU-5 for equimolar C_2H_2/CO_2 (50/50) mixture. As shown in Fig. 6, ZNU-5 exhibits a stepped breakthrough curve for C_2H_2, which is not seen in rigid adsorbents [54]. Nonetheless, the captured C_2H_2 amount is still very large while that of CO_2 is negligible, thus leading to a high separation factor. Besides, as C_2H_2, the target gas, needs desorption process to obtain, slight leakage in the breakthrough process will not have large influence on the dynamic capacity of C_2H_2.

To evaluate the practical separation performance as well as confirm the stepped breakthrough phenomenon, experimental breakthrough tests were conducted. The results showed that the experimental breakthrough curves are very similar with the simulations (Fig. S18 in the ESM). For equimolar C_2H_2/CO_2 mixtures, efficient separations could be accomplished by ZNU-5

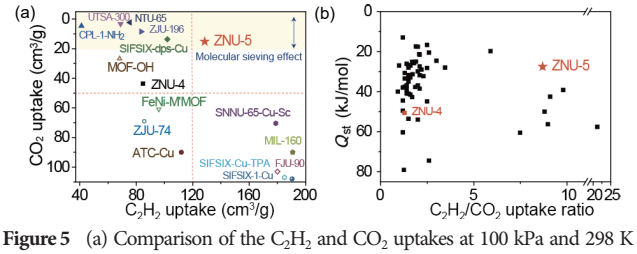

Figure 5 (a) Comparison of the C_2H_2 and CO_2 uptakes at 100 kPa and 298 K between ZNU-5 and other materials. (b) Comparison of C_2H_2/CO_2 uptake ratio and Q_{st} for C_2H_2 between ZNU-5 and other materials.

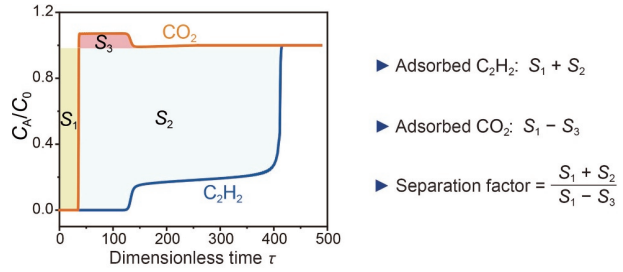

Figure 6 Simulated breakthrough curve of ZNU-5 for C_2H_2/CO_2 (50/50) at 298 K.

with 3.3 mol/g of C_2H_2 capacity, while the uptake of C_2H_2 absorbed in ZNU-4 was only 2.2 mol/g (Fig. 7(a)). Subsequently, we explored the effect of different desorption temperatures on regeneration. Figure 7(b) shows that the desorption time of C_2H_2 is gradually shortened with the increase of desorption temperature. Controlling the desorption temperature of 25 °C, 2.6 mol/g of 98% purity C_2H_2 can be recovered from the column after blowing CO_2 out at the first stage. The dynamic separation factor of C_2H_2/CO_2 is calculated to be 9.1 (Fig. S20 in the ESM), higher than those of ZNU-4 (5.4) [34] and many other top-performing materials such as CAU-10-H (3.4) [53] , JCM-1 (4.4) [45], ZJU-74a (4.3) [55], and SNNU-45 (2.9) [8]. The capture ability of ZNU-5 for C_2H_2 from the ternary and quaternary mixtures was further studied. As shown in Figs. 7(c) and 7(d), when the gas mixtures containing equal ratios of $C_2H_2/CO_2/CH_4$ or $C_2H_2/CO_2/CH_4/C_2H_4$ passed through the ZNU-5 packed column, CO_2/CH_4 or $CO_2/CH_4/C_2H_4$ outflowed first, then C_2H_2 began to discharge at around 104/170 min, and up to 2.8/2.2 mmol/g of C_2H_2 was adsorbed in this process. During desorption process, 2.0/1.5 mmol/g of 98% purity C_2H_2 can be recovered from the column by stepped Ar purge process, which are both higher than those of ZNU-4 (0.48 and 0.05 mmol/g) [34].

Recycability is a very important parameter to assess the potential for practical application. Thus, 5 repetitive breakthrough experiments were carried out. Negligible capacity reduction is observed (Fig. 8), demonstrating that ZNU-5 is a promising adsorbent with good cyclic utilization performance.

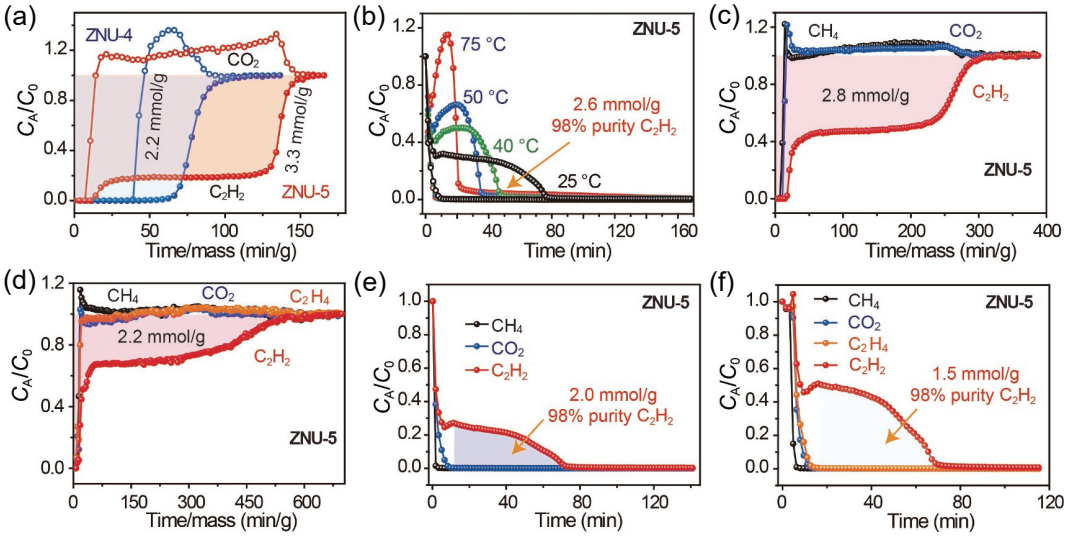

Figure 7 (a) The breakthrough curve for C_2H_2/CO_2 (50/50) separation at ZNU-4 and ZNU-5. (b) The C_2H_2/CO_2 (50/50) desorption curves for ZNU-5 at 25, 40, 50, and 75 °C. (c) The breakthrough curve for $C_2H_2/CO_2/CH_4$ (33.3/33.3/33.3) separation at ZNU-5. (d) The breakthrough curves for $C_2H_2/CO_2/C_2H_4/CH_4$ (25/25/25/25) separation at ZNU-5. (e) The desorption curves for $C_2H_2/CO_2/CH_4$ (33.3/33.3/33.3) separation at ZNU-5. (f) The desorption curves for $C_2H_2/CO_2/C_2H_4/CH_4$ (25/25/25/25) separation at ZNU-5.

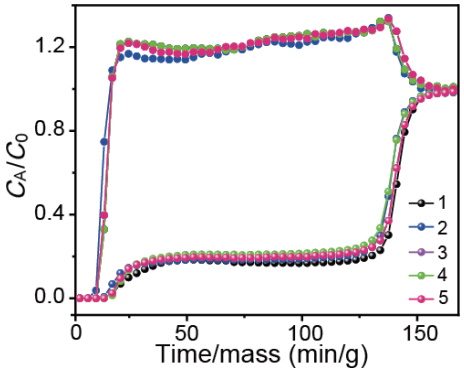

Figure 8 Five cycles of dynamic breakthrough curves for C_2H_2/CO_2 (50/50, v/v) mixture.

4 Conclusions

In a nutshell, we reported a novel fluorinated anion pillared MOF with flexible molecular sieving effect that can efficiently capture C_2H_2 from CO_2 and C_nH_4 (n = 1 and 2). The foregoing results revealed that ZNU-5 exhibits not only high C_2H_2 uptake capacity but also simultaneously excellent C_2H_2/CO_2 (12), C_2H_2/C_2H_4 (255), and C_2H_2/CH_4 (850) selectivity under ambient conditions, outperforming most of the flexible molecular sieving MOFs reported. Experimental breakthrough tests further confirmed the effective capture of C_2H_2 from binary C_2H_2/CO_2, ternary $C_2H_2/CO_2/CH_4$, and quaternary $C_2H_2/CO_2/CH_4/C_2H_4$ mixtures with large productivity and good recycability. Thus, combining large working capacity, low adsorption heat, as well as excellent recyclability, ZNU-5 is a promising adsorbent for practical C_2H_2 purification and separation. The mechanism of the selective gate opening behavior is under study.

Acknowledgements

Y. B. Z. acknowledged the financial support by the National Natural Science Foundation of China (No. 21908193) and Jinhua Industrial Key Project (No. 2021A22648). S. D. acknowledged the financial support by the National Natural Science Foundation of China (No. 21871231) and the Special Funds for Basic Scientific Research of Zhejiang University (Nos. 2019QNA3010 and K20210335). L. Y. W. acknowledged the financial support by the

National Natural Science Foundation of China (No. 22205207).

Electronic Supplementary Material: Supplementary material (crystallographic data and additional figures) is available in the online version of this article at https://doi.org/10.1007/s12274-022-4996-9.

References

[1] Weissermel, K.; Arpe, H. J. *Industrial Organic Chemistry*, 4th ed.; Wiley-VCH: Weinheim, 2003.

[2] Zhang, Y. B.; Hu, J. B.; Krishna, R.; Wang, L. Y.; Yang, L. F.; Cui, X. L.; Duttwyler, S.; Xing, H. B. Rational design of microporous MOFs with anionic boron cluster functionality and cooperative dihydrogen binding sites for highly selective capture of acetylene. *Angew. Chem., Int. Ed.* **2020**, *59*, 17664–17669.

[3] Moreau, F.; da Silva, I.; Al Smail, N. H.; Easun, T. L.; Savage, M.; Godfrey, H. G. W.; Parker, S. F.; Manuel, P.; Yang, S. H.; Schröder, M. Unravelling exceptional acetylene and carbon dioxide adsorption within a tetra-amide functionalized metal-organic framework. *Nat. Commun.* **2017**, *8*, 14085.

[4] Fan, W. D.; Wang, X.; Liu, X. P.; Xu, B.; Zhang, X. R.; Wang, W. J.; Wang, X. K.; Wang, Y. T.; Dai, F. N.; Yuan, D. Q. et al. Regulating C_2H_2 and CO_2 storage and separation through pore environment modification in a microporous Ni-MOF. *ACS Sustainable Chem. Eng.* **2019**, *7*, 2134–2140.

[5] Wang, G. D.; Wang, H. H.; Shi, W. J.; Hou, L.; Wang, Y. Y.; Zhu, Z. H. A highly stable MOF with F and N accessible sites for efficient capture and separation of acetylene from ternary mixtures. *J. Mater. Chem. A* **2021**, *9*, 24495–24502.

[6] Foo, M. L.; Matsuda, R.; Hijikata, Y.; Krishna, R.; Sato, H.; Horike, S.; Hori, A.; Duan, J. G.; Sato, Y.; Kubota, Y. et al. An adsorbate discriminatory gate effect in a flexible porous coordination polymer for selective adsorption of CO_2 over C_2H_2. *J. Am. Chem. Soc.* **2016**, *138*, 3022–3030.

[7] Wang, Q. J.; Hu, J. B.; Yang, L. F.; Zhang, Z. Q.; Ke, T.; Cui, X. L.; Xing, H. B. One-step removal of alkynes and propadiene from cracking gases using a multi-functional molecular separator. *Nat. Commun.* **2022**, *13*, 2955.

[8] Li, Y. P.; Wang, Y.; Xue, Y. Y.; Li, H. P.; Zhai, Q. G.; Li, S. N.; Jiang, Y. C.; Hu, M. C.; Bu, X. H. Ultramicroporous building units as a path to Bi-microporous metal-organic frameworks with high acetylene storage and separation performance. *Angew. Chem., Int. Ed.* **2019**, *58*, 13590–13595.

[9] Niu, Z.; Cui, X. L.; Pham, T.; Verma, G.; Lan, P. C.; Shan, C.; Xing, H. B.; Forrest, K. A.; Suepaul, S.; Space, B. et al. A MOF-based ultra-strong acetylene nano-trap for highly efficient C_2H_2/CO_2 separation. *Angew. Chem., Int. Ed.* **2021**, *60*, 5283–5288.

[10] Zhang, L.; Jiang, K.; Yang, L. F.; Li, L. B.; Hu, E. L.; Yang, L.; Shao, K.; Xing, H. B.; Cui, Y. J.; Yang, Y. et al. Benchmark C_2H_2/CO_2 separation in an ultra-microporous metal-organic framework via copper(I)-alkynyl chemistry. *Angew. Chem., Int. Ed.* **2021**, *60*, 15995–16002.

[11] Sun, W. Q.; Hu, J. B.; Jiang, Y. J.; Xu, N.; Wang, L. Y.; Li, J. H.; Hu, Y. Q.; Duttwyler, S.; Zhang, Y. B. Flexible molecular sieving of C_2H_2 from CO_2 by a new cost-effective metal organic framework with intrinsic hydrogen bonds. *Chem. Eng. J.* **2022**, *439*, 135745.

[12] Di, Z. Y.; Pang, J. D.; Hu, F. L.; Wu, M. Y.; Hong, M. C. An ultra-stable microporous supramolecular framework with highly selective adsorption and separation of water over ethanol. *Nano Res.* **2021**, *14*, 2584–2588.

[13] Fan, W. D.; Yuan, S.; Wang, W. J.; Feng, L.; Liu, X. P.; Zhang, X. R.; Wang, X.; Kang, Z. X.; Dai, F. N.; Yuan, D. Q. et al. Optimizing multivariate metal-organic frameworks for efficient C_2H_2/CO_2 separation. *J. Am. Chem. Soc.* **2020**, *142*, 8728–8737.

[14] Liu, Y.; Xu, Q. Q.; Chen, L. H.; Song, C. H.; Yang, Q. W.; Zhang, Z. G.; Lu, D.; Yang, Y. W.; Ren, Q. L.; Bao, Z. B. Hydrogen-bonded metal-nucleobase frameworks for highly selective capture of ethane/propane from methane and methane/nitrogen separation. *Nano Res.* **2022**, *15*, 7695–7702.

[15] Chen, S.; Behera, N.; Yang, C.; Dong, Q. B.; Zheng, B. S.; Li, Y. Y.; Tang, Q.; Wang, Z. X.; Wang, Y. Q.; Duan, J. G. A chemically stable nanoporous coordination polymer with fixed and free Cu^{2+} ions for boosted C_2H_2/CO_2 separation. *Nano Res.* **2021**, *14*, 546–553.

[16] Cui, J. Y.; Zhang, Z. Q.; Tan, B.; Zhang, Y. B.; Wang, P. C.; Cui, X. L.; Xing, H. B. Efficient separation of n-butene and iso-butene by flexible ultramicroporous metal-organic frameworks with pocket-like cavities. *Chem.—Asian J.* **2019**, *14*, 3572–3576.

[17] Fu, X. P.; Wang, Y. L.; Zhang, X. F.; Krishna, R.; He, C. T.; Liu, Q. Y.; Chen, B. L. Collaborative pore partition and pore surface fluorination within a metal-organic framework for high-performance C_2H_2/CO_2 separation. *Chem. Eng. J.* **2022**, *432*, 134433.

[18] Duan, J. G.; Higuchi, M.; Zheng, J. J.; Noro, S. I.; Chang, I. Y.; Hyeon-Deuk, K.; Mathew, S.; Kusaka, S.; Sivaniah, E.; Matsuda, R. et al. Density gradation of open metal sites in the mesospace of porous coordination polymers. *J. Am. Chem. Soc.* **2017**, *139*, 11576–11583.

[19] Sharma, S.; Mukherjee, S.; Desai, A. V.; Vandichel, M.; Dam, G. K.; Jadhav, A.; Kociok-Köhn, G.; Zaworotko, M. J.; Ghosh, S. K. Efficient capture of trace acetylene by an ultramicroporous metal-organic framework with purine binding sites. *Chem. Mater.* **2021**, *33*, 5800–5808.

[20] Sun, W. Q.; Hu, J. B.; Duttwyler, S.; Wang, L. Y.; Krishna, R.; Zhang, Y. B. Highly selective gas separation by two isostructural boron cluster pillared MOFs. *Sep. Purif. Technol.* **2022**, *283*, 120220.

[21] Wang, G. D.; Li, Y. Z.; Zhang, W. F; Hou, L.; Wang, Y. Y.; Zhu, Z. H. Acetylene separation by a Ca-MOF containing accessible sites of open metal centers and organic groups. *ACS Appl. Mater. Interfaces* **2021**, *13*, 58862–58870.

[22] Yang, L. F.; Qian, S. H.; Wang, X. B.; Cui, X. L.; Chen, B. L.; Xing, H. B. Energy-efficient separation alternatives: Metal-organic frameworks and membranes for hydrocarbon separation. *Chem. Soc. Rev.* **2020**, *49*, 5359–5406.

[23] Zhang, Y. B.; Cui, X. L.; Xing, H. B. Recent advances in the capture and abatement of toxic gases and vapors by metal-organic frameworks. *Mater. Chem. Front.* **2021**, *5*, 5970–6013.

[24] Zhang, Z.; Peh, S. B.; Wang, Y. X.; Kang, C. J.; Fan, W. D.; Zhao, D. Efficient trapping of trace acetylene from ethylene in an ultramicroporous metal-organic framework: Synergistic effect of high-density open metal and electronegative sites. *Angew. Chem., Int. Ed.* **2020**, *59*, 18927–18932.

[25] Fan, W. D.; Wang, X.; Zhang, X. R.; Liu, X. P.; Wang, Y. T.; Kang, Z. X.; Dai, F. N.; Xu, B.; Wang, R. M.; Sun, D. F. Fine-tuning the pore environment of the microporous Cu-MOF for high propylene storage and efficient separation of light hydrocarbons. *ACS Cent. Sci.* **2019**, *5*, 1261–1268.

[26] Zeng, H.; Xie, M.; Huang, Y. L.; Zhao, Y. F.; Xie, X. J.; Bai, J. P.; Wan, M. Y.; Krishna, R.; Lu, W. G.; Li, D. Induced fit of C_2H_2 in a flexible MOF through cooperative action of open metal sites. *Angew. Chem., Int. Ed.* **2019**, *58*, 8515–8519.

[27] Fan, W. D.; Ying, Y. P.; Peh, S. B.; Yuan, H. Y.; Yang, Z. Q.;Yuan, Y. D.; Shi, D. C.; Yu, X.; Kang, C. J.; Zhao, D. Multivariate polycrystalline metal-organic framework membranes for CO_2/CH_4 separation. *J. Am. Chem. Soc.* **2021**, *143*, 17716–17723.

[28] Jiang, Y. J.; Hu, J. B.; Wang, L. Y.; Sun, W. Q.; Xu, N.; Krishna, R.; Duttwyler, S.; Cui, X. L.; Xing, H. B.; Zhang, Y. B. Comprehensive pore tuning in an ultrastable fluorinated anion cross-linked cage-like MOF for simultaneous benchmark propyne recovery and propylene purification. *Angew. Chem., Int. Ed.* **2022**, *61*, e202200947.

[29] Li, S. L.; Zeng, S. L.; Tian, Y. Y.; Jing, X. F.; Sun, F. X.; Zhu, G. S. Two flexible cationic metal-organic frameworks with remarkable stability for CO_2/CH_4 separation. *Nano Res.* **2021**, *14*, 3288–3293.

[30] Wang, L. Y.; Jiang, T.; Duttwyler, S.; Zhang, Y. B. Supramolecular Cu(II)-dipyridyl frameworks featuring weakly coordinating dodecaborate dianions for selective gas separation. *CrystEngComm* **2021**, *23*, 282–291.

[31] Lin, R. B.; Li, L. B.; Wu, H.; Arman, H.; Li, B.; Lin, R. G.; Zhou, W.; Chen, B. L. Optimized separation of acetylene from carbon dioxide and ethylene in a microporous material. *J. Am. Chem. Soc.*

2017, *139*, 8022–8028.
[32] Wang, J.; Zhang, Y.; Su, Y.; Liu, X.; Zhang, P. X.; Lin, R. B.; Chen, S. X.; Deng, Q.; Zeng, Z. L.; Deng, S. G. et al. Fine pore engineering in a series of isoreticular metal-organic frameworks for efficient C_2H_2/CO_2 separation. *Nat. Commun.* **2022**, *13*, 200.
[33] Wang, L. Y.; Sun, W. Q.; Zhang, Y. B.; Xu, N.; Krishna, R.; Hu, J. B.; Jiang, Y. J.; He, Y. B.; Xing, H. B. Interpenetration symmetry control within ultramicroporous robust boron cluster hybrid MOFs for benchmark purification of acetylene from carbon dioxide. *Angew. Chem., Int. Ed.* **2021**, *60*, 22865–22870.
[34] Xu, N.; Hu, J. B.; Wang, L. Y.; Luo, D.; Sun, W. Q.; Hu, Y. Q.; Wang, D. M.; Cui, X. L.; Xing, H. B.; Zhang, Y. B. A TIFSIX pillared MOF with unprecedented zsd topology for efficient separation of acetylene from quaternary mixtures. *Chem. Eng. J.* **2022**, *450*, 138034.
[35] Dong, Q. B.; Zhang, X.; Liu, S.; Lin, R. B.; Guo, Y. N.; Ma, Y. S.; Yonezu, A.; Krishna, R.; Liu, G. P.; Duan, J. G. et al. Tuning gate-opening of a flexible metal-organic framework for ternary gas sieving separation. *Angew. Chem., Int. Ed.* **2020**, *59*, 22756–22762.
[36] Zhang, L.; Jiang, K.; Li, L. B.; Xia, Y. P.; Hu, T. L.; Yang, Y.; Cui, Y. J.; Li, B.; Chen, B. L.; Qian, G. D. Efficient separation of C_2H_2 from C_2H_2/CO_2 mixtures in an acid-base resistant metal-organic framework. *Chem. Commun.* **2018**, *54*, 4846–4849.
[37] Yang, L. Z.; Yan, L. T.; Wang, Y.; Liu, Z.; He, J. X.; Fu, Q. J.; Liu, D. D.; Gu, X.; Dai, P. C.; Li, L. J.; Zhao, X. B. Adsorption site selective occupation strategy within a metal-organic framework for highly efficient sieving acetylene from carbon dioxide. *Angew. Chem., Int. Ed.* **2021**, *60*, 4570–4574.
[38] Gong, W.; Cui, H.; Xie, Y.; Li, Y. G.; Tang, X. H.; Liu, Y.; Cui, Y.; Chen, B. L. Efficient C_2H_2/CO_2 separation in ultramicroporous metal-organic frameworks with record C_2H_2 storage density. *J. Am. Chem. Soc.* **2021**, *143*, 14869–14876.
[39] Zhang, J. W.; Hu, M. C.; Li, S. N.; Jiang, Y. C.; Qu, P.; Zhai, Q. G. Assembly of $[Cu_2(COO)_4]$ and $[M_3(\mu_3\text{-}O)(COO)_6]$ (M = Sc, Fe, Ga, and In) building blocks into porous frameworks towards ultra-high C_2H_2/CO_2 and C_2H_2/CH_4 separation performance. *Chem. Commun.* **2018**, *54*, 2012–2015.
[40] Ye, Y. X.; Xian, S. K.; Cui, H.; Tan, K.; Gong, L. S.; Liang, B.; Pham, T.; Pandey, H.; Krishna, R.; Lan, P. C. et al. Metal-organic framework based hydrogen-bonding nanotrap for efficient acetylene storage and separation. *J. Am. Chem. Soc.* **2022**, *144*, 1681–1689.
[41] Ye, Y. X.; Ma, Z. L.; Lin, R. B.; Krishna, R.; Zhou, W; Lin, Q. J.; Zhang, Z. J.; Xiang, S. C.; Chen, B. L. Pore space partition within a metal-organic framework for highly efficient C_2H_2/CO_2 separation. *J. Am. Chem. Soc.* **2019**, *141*, 4130–4136.
[42] Li, H.; Liu, C. P.; Chen, C.; Di, Z. Y.; Yuan, D. Q.; Pang, J. D.; Wei, W.; Wu, M. Y.; Hong, M. C. An unprecedented pillar-cage fluorinated hybrid porous framework with highly efficient acetylene storage and separation. *Angew. Chem., Int. Ed.* **2021**, *60*, 7547–7552.
[43] Cui, X. L.; Chen, K. J.; Xing, H. B.; Yang, Q. W.; Krishna, R.; Bao, Z. B.; Wu, H.; Zhou, W.; Dong, X. L.; Han, Y. et al. Pore chemistry and size control in hybrid porous materials for acetylene capture from ethylene. *Science.* **2016**, *353*, 141–144.
[44] Dutta, S.; Mukherjee, S.; Qazvini, O. T.; Gupta, A. K.; Sharma, S.; Mahato, D.; Babarao, R.; Ghosh, S. K. Three-in-one C_2H_2-selectivity-guided adsorptive separation across an isoreticular family of cationic square-lattice MOFs. *Angew. Chem., Int. Ed.* **2022**, *61*, e202114132.
[45] Lee, J.; Chuah, C. Y.; Kim, J.; Kim, Y.; Ko, N.; Seo, Y.; Kim, K.; Bae, T. H.; Lee, E. Separation of acetylene from carbon dioxide and ethylene by a water-stable microporous metal-organic framework with aligned imidazolium groups inside the channels. *Angew. Chem., Int. Ed.* **2018**, *57*, 7869–7873.
[46] Mukherjee, S.; He, Y. H.; Franz, D.; Wang, S. Q.; Xian, W. R.; Bezrukov, A. A.; Space, B.; Xu, Z. T.; He, J.; Zaworotko, M. J. Halogen-C_2H_2 binding in ultramicroporous metal-organic frameworks (MOFs) for benchmark C_2H_2/CO_2 separation selectivity. *Chem.—Eur. J.* **2020**, *26*, 4923–4929.
[47] Zhao, J. Y.; Li, Q.; Zhu, X. C.; Li, J.; Wu, D. P. Highly robust tetranuclear cobalt-based 3D framework for efficient C_2H_2/CO_2 and C_2H_2/C_2H_4 separations. *Inorg. Chem.* **2020**, *59*, 14424–14431.
[48] Meng, L. K.; Yang, L. X.; Chen, C. L.; Dong, X. L.; Ren, S. Y.; Li, G. H.; Li, Y.; Han, Y.; Shi, Z.; Feng, S. H. Selective acetylene adsorption within an imino-functionalized nanocage-based metal-organic framework. *ACS Appl. Mater. Interfaces* **2020**, *12*, 5999–6006.
[49] Peng, Y. L.; Pham, T.; Li, P. F.; Wang, T.; Chen, Y.; Chen, K. J.; Forrest, K. A.; Space, B.; Cheng, P.; Zaworotko, M. J. et al. Robust ultramicroporous metal-organic frameworks with benchmark affinity for acetylene. *Angew. Chem., Int. Ed.* **2018**, *57*, 10971–10975.
[50] Zhang, J. P.; Chen, X. M. Optimized acetylene/carbon dioxide sorption in a dynamic porous crystal. *J. Am. Chem. Soc.* **2009**, *131*, 5516–5521.
[51] Zhang, X.; Lin, R. B.; Wu, H.; Huang, Y. H.; Ye, Y. X.; Duan, J. G.; Zhou, W.; Li, J. R.; Chen. B. L. Maximizing acetylene packing density for highly efficient C_2H_2/CO_2 separation through immobilization of amine sites within a prototype MOF. *Chem. Eng. J.* **2022**, *431*, 134184.
[52] Zhang, Y. B.; Wang, L. Y.; Hu, J. B.; Duttwyler, S.; Cui, X. L.; Xing, H. B. Solvent-dependent supramolecular self-assembly of boron cage pillared metal-organic frameworks for selective gas separation. *CrystEngComm* **2020**, *22*, 2649–2655.
[53] Pei, J. Y.; Wen, H. M.; Gu, X. W.; Qian, Q. L.; Yang, Y.; Cui, Y. J.; Li, B.; Chen, B. L.; Qian, G. D. Dense packing of acetylene in a stable and low-cost metal-organic framework for efficient C_2H_2/CO_2 separation. *Angew. Chem., Int. Ed.* **2021**, *60*, 25068–25074.
[54] Sotomayor, F. J.; Lastoskie, C. M. Predicting the breakthrough performance of "gating" adsorbents using osmotic framework-adsorbed solution theory. *Langmuir* **2017**, *33*, 11670–11678.
[55] Pei, J. Y.; Shao, K.; Wang, J. X.; Wen, H. M.; Yang, Y.; Cui, Y. J.; Krishna, R.; Li, B.; Qian, G. D. A chemically stable hofmann-type metal-organic framework with sandwich-like binding sites for benchmark acetylene capture. *Adv. Mater.* **2020**, *32*, 1908275.